2012 Hawaii University International Conferences
Education, Math & Engineering Technology
July 31st to August 2nd
Waikiki Beach Marriot Resort & Spa
Honolulu, Hawaii

Geometric Power Series In Action

Mulatu Lemma and Travis Young
MAGEC-STEM Plus
NSF Program
Savannah State University
Savannah, Georgia 31404

An Accurate Experimental Method For Determining Mode One Stress Intensity Factor

Nash Younis

Professor of Mechanical Engineering

younis@engr.ipfw.edu

Department of Engineering
Indiana University – Purdue University Fort Wayne
Fort Wayne, Indiana 46805-1499, USA

NOTATION

a	crack length, hole radius
A	cross sectional area
C	stress optical constant
d	thickness of specimen
D_{max}	caustic's maximum diameter
F	Axial force
Z_i	distance between the divergent light source and the model
Z_o	distance between model and screen
W	plate width
σ	applied stress
σ_x, σ_y	Plane Cartesian stress components
σ_r, σ_θ	Plane polar stress components
λ	magnification factor

ABSTRACT

Mathematics and engineering optics are correlated seeing that the literature is inconclusive in regard to selecting the maximum diameter of the reflected caustics image. An experimental investigation was performed to establish the effects of diffraction on the determination of stress intensity factors utilizing the method of reflected caustics. Mathematical reflected caustics from the front and rear face of a transparent material were generated and validated by experiment. The study introduces the reflected caustics from the rear face of a plate with a circular hole as a calibration method. The accuracy of the proposed calibration technique is demonstrated by comparing experimental results to theory.

INRTODUCTION

The experimental optical method of caustics was established for solving the singularity at the crack tip by evaluating mode I stress intensity factor (SIF) under static and dynamic loading. Manogg [1] introduced the method of transmitted caustics and Theocaris [2] introduced the method of reflected caustics. The method is one of the few experimental methods which provide applicable results in regions with high stress gradients. Thus, it is applicability was gradually extended for the solution of other engineering problems that deal with stress concentration. For example, the method was extended to the analysis of contact problems for mechanically isotropic [3] and anisotropic materials [4]. Spitas et al. used the method to measure the contact of gear tooth pairs in mesh [5].

In the last decade, the main emphasis is extended to study dynamic fracture of anisotropic material and dynamic propagation of multi-cracks and interface cracks in practical engineering materials. Researchers have compared the method to other experimental techniques and concluded that it is a powerful method to solve statics as well as dynamics fracture problems. In 2011, Yao and Xu [6] reviewed the recent advances and applications about the dynamic caustic method such as impact response and dynamic fracture of composite materials.

Stress Intensity Factor

Due to the high stress concentration in the region surrounding the crack tip, both the thickness and the refractive index of the materials change. As a consequence, the area surrounding the crack tip acts similar to divergent lens. The caustic is the image of a circular line on the specimen centered at the crack tip, which is called the initial curve. While the method is simple for determining SIF, special precautions should be taken so that correct evaluation equation are used. Sources of experimental error such as the quality of the incident beam, specimen surface preparation and the alignment of the specimen loading fixture were considered in the study by Wallhead et al. [7]. Incorrect experimental measurements, utilizing reflected caustics, are also discussed in relation to the resulting error for evaluating the crack tip stress intensity factor [8]

When the initial curve is inside the region where the stress state is predominately three-dimensional, the simple caustic equations are not valid [9]. It was found that the values of the stress intensity factor K_I, which were based on the diameters of the caustics, were varied with the load, the crack length and the caustic shape because the caustic becomes oval in higher loads or higher crack length. Thus, in 2011 Papadopoulos proposed a new formula for calculating K_I depending on the area of caustic [10]. Due to the diffraction effects, the literature is inconclusive about the measurement of the maximum diameter of the transmitted caustic [11]. Tomlinson and Patterson [12] investigated the effects of curvature on the SIF determined from reflected caustics. They found that relatively small surface curvatures caused significant errors in the stress intensity factor.

Holes

In the case of a uniaxially loaded perforated plate, the method of caustics had been used for the experimental determination of the difference of the remotely applied stresses. This is not a practical approach considering other experimental stress analysis techniques. However, the application of the caustics images in a plate with a circular hole was extended for determining some materials properties. For example, Younis utilized the transmitted and reflected caustic for the determination of some mechanical properties [13]. Some critical points related to the applicability of the optical method of reflected caustics in the case of a plate with a central hole were explored in 2011 [14]. The defined critical distance was correlated with the condition, which influence the caustic, thus the range of applicability of the method of caustic around hole was defined [15]. The validity of this range was experimentally checked.

PROBLEM STATEMENT

Theoretically, the reflected from the rear face caustic band can be located at the transition from the inner dark space to bright rim. Except for the diffraction effects, the caustic band has a finite width and herein lies the measurement problem. This causes uncertainty in selecting the maximum diameter. Thus, in this study the stress optical constant is determined using the reflected caustic [16] and its value used in calculating K_I utilizing the same method. Accounting for the diffraction effects, the results obtained based on the proposed technique show that the results of determining K_I can be enhanced considerably. This article deals with the reflected from rear face caustic and the reflected one from the front face is beyond the scope of this study.

MATHEMATICS AND MECHANICS

The advantage of reflected caustics relative to other optical experimental techniques is that the same equipment can be used in either a reflection or a transmission arrangement. In addition, the application of the reflected caustics is more practical than that of the transmitted one in the engineering field. The principle of the method is simple in concept. The formation of the caustics image is dependent on the stresses in a structural member or machine component. Therefore, it is an ideal method to be used for when there is a stress concentration factor (holes) or SIF (cracks) since high stress gradients produce large deflection of the light rays and an image with distinguishing characteristics.

Consider an edge crack of length a, or a small circular hole of radius a, in an infinite plate under uniform unidirectional tension σ = F/A as shown in figures 1 and 2. The theory of elasticity solution for edge crack [17] and central hole [18] in an infinite plate is:

Table 1: Stress fields equations

Edge Crack	Circular Hole
$\boldsymbol{\sigma_x = \frac{K_I}{\sqrt{2\pi r}}\left(1 - sin\frac{\theta}{2} sin\frac{3\theta}{2}\right) cos\frac{\theta}{2}}$	$\sigma_r = \frac{\sigma}{2}\left\{\left(1-\frac{a^2}{r^2}\right)\left[1+\left(\frac{3a^2}{r^2}-1\right)\cos 2\theta\right]\right\}$
$\boldsymbol{\sigma_y = \frac{K_I}{\sqrt{2\pi r}}\left(1 + sin\frac{\theta}{2} sin\frac{3\theta}{2}\right) cos\frac{\theta}{2}}$	$\sigma_\theta = \frac{\sigma}{2}\left[\left(1+\frac{a^2}{r^2}\right)+\left(\frac{3a^4}{r^4}+1\right)\cos 2\theta\right]$
$\boldsymbol{\tau_{xy} = \frac{K_I}{\sqrt{2\pi r}}\, sin\frac{\theta}{2} cos\frac{3\theta}{2}\, cos\frac{\theta}{2}}$	$\tau_{r\theta} = \frac{\sigma}{2}\left[\left(1+\frac{3a^2}{r^2}\right)\left(1-\frac{a^2}{r^2}\right)\sin 2\theta\right]$

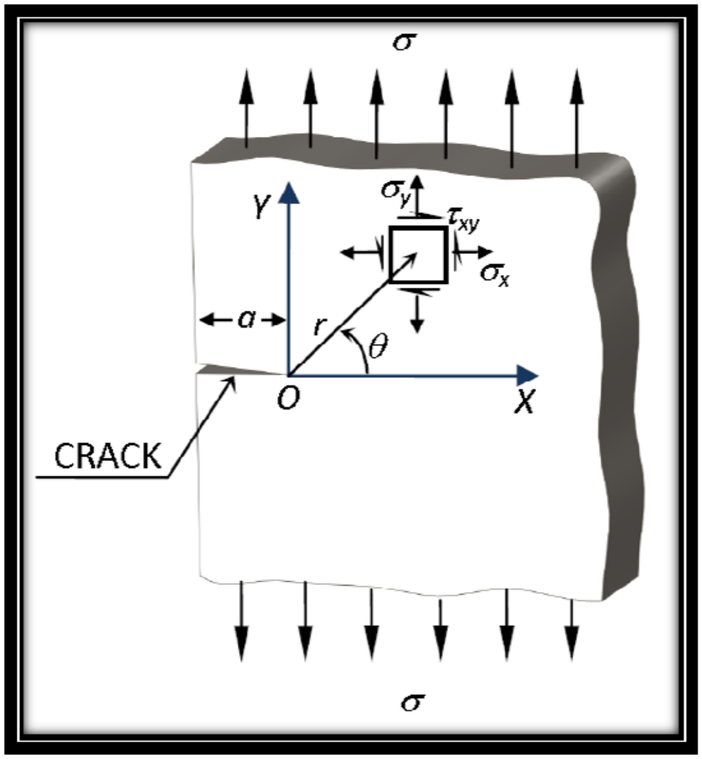

Figure 1 Edge crack in an infinite plate subjected to a remote tensile stress

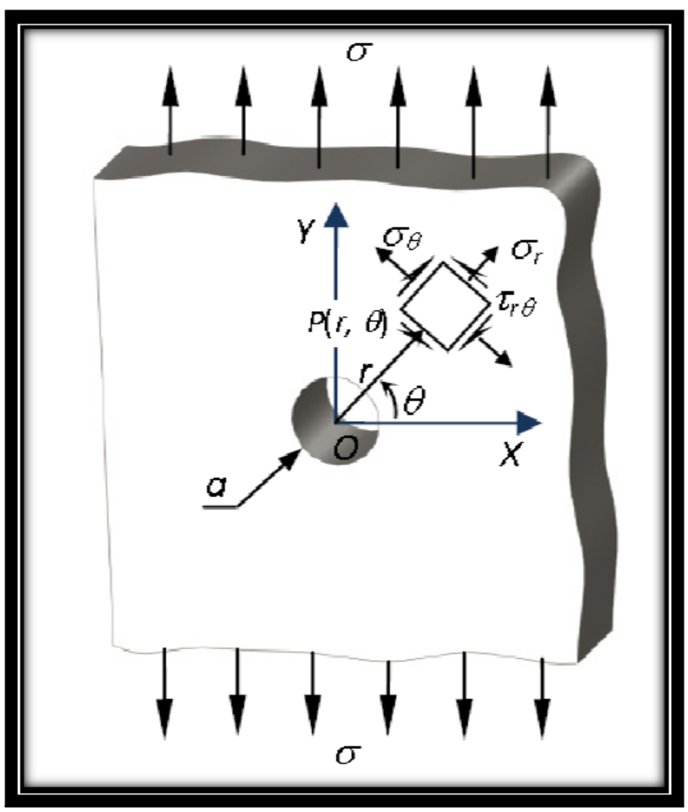

Figure 2 Central hole in an infinite plate subjected to a remote tensile stress

Stresses in a solid alter the optical properties of the solid. These changes in the optical properties are utilized in the method of caustics. Due to the high stress concentration in the region surrounding the hole/crack, both the thickness and refractive index (hence the optical path) of the material will change. The changes in the thickness and optical path are [19]:

$$\Delta_d = \frac{\nu}{E}(\sigma_1 + \sigma_2)d \tag{1}$$

$$\Delta_s = cd\,(\sigma_1 + \sigma_2) \tag{2}$$

From the stress fields in the Table 1, the sum of the in-plane principal stresses is shown in Table 2 (equation 3).

MATHEMATICS AND OPTICAL ENGINEERING

As a result of the high stress in the vicinity of the crack tip/hole, the area acts similar to a divergent lens. The deviation vector D is shown in Fig. 3. The direction and magnitude of the deviation vector are correlated to the change in the optical path Δs and it is given by the eikonal equation [20] as:

$$\mathrm{D} = \mathrm{Z_o}\,\mathrm{grad}\,\Delta_\mathrm{s} \tag{4}$$

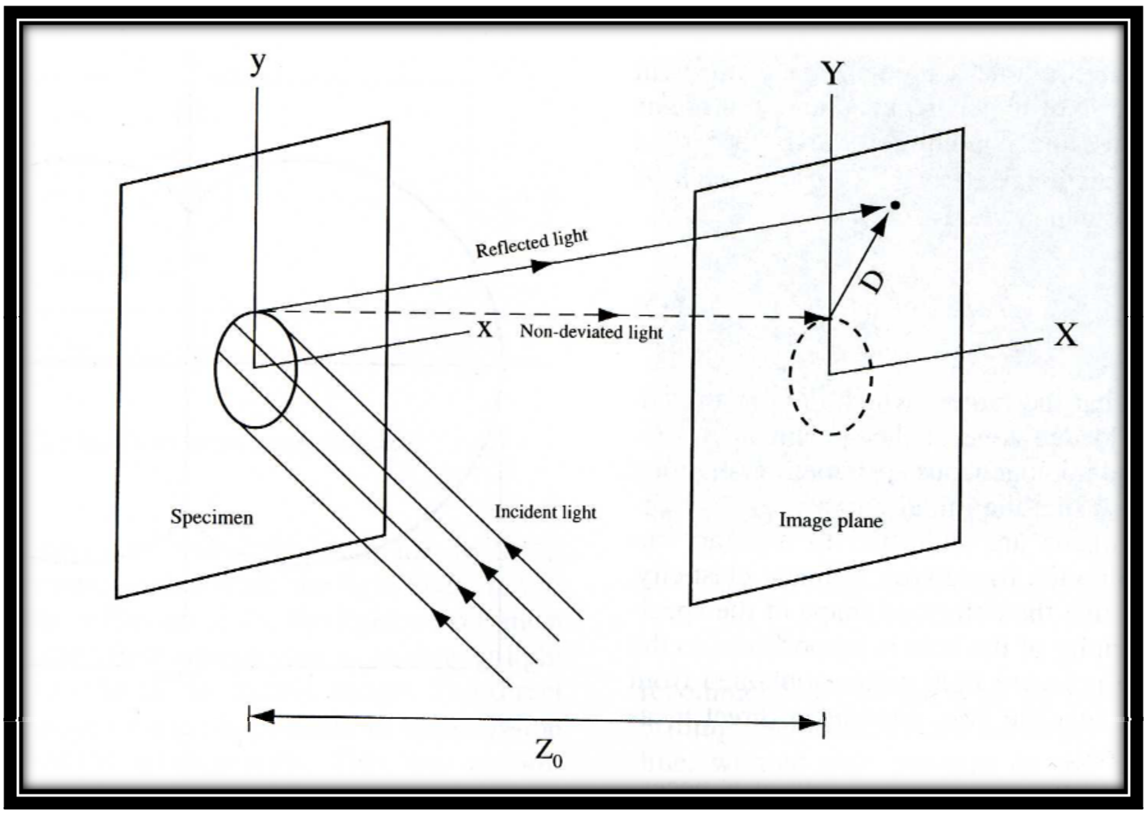

Figure 3 Mapping of the object plane onto the image plane

Substituting the sum of principal stresses (equation 3) into equations 1&2; and then the results into equation 4 yields equation (5). The mapping of the specimen plane on the image plane is shown in Fig. 4. The point p is placed in a local region near the hole (or edge crack). However, after propagating down the optical bench, the deflected light ray impinges the screen at point p' whose location is given by the vector r'. The image vector equation can be written as:

$$\boldsymbol{r}^{/} = \boldsymbol{r} + \boldsymbol{D} \tag{7}$$

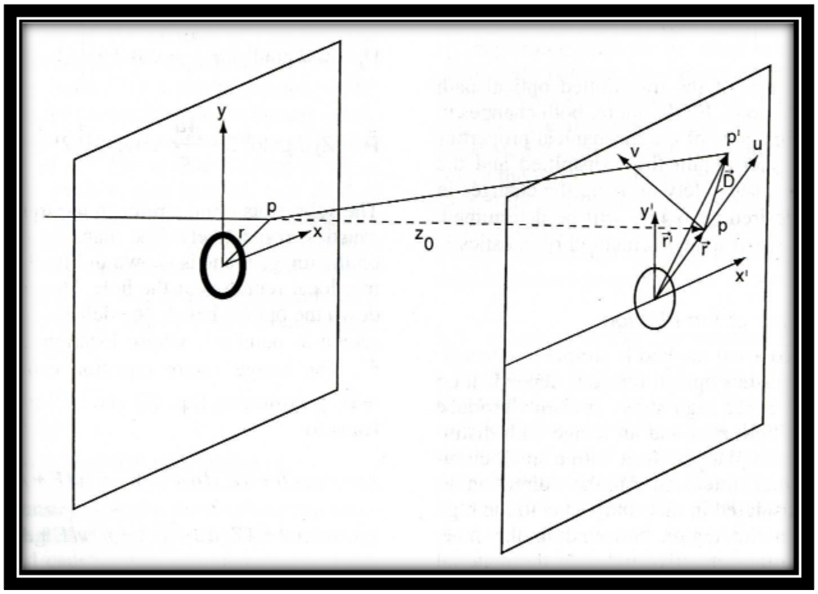

Figure 4 Geometrical conditions of the reflected caustic analysis

From eqs. (5) and (7), the vector $\boldsymbol{r}^{/}$ in the Cartesian coordinates (x, y) is shown in equation (8) for both singularities. The complete family of the deflected light rays forms a shadow space in front of the object plane. Its surface is an envelope to the light rays and is called the caustic surface. The intersection of this surface with the image plane forms the caustic curve. This caustic curve is multi-valued, singular solution of eqs. (4) and (7). Since the mapping along the caustic curve is not reversible, the sufficient condition for the existence of the caustic curve is obtained if the Jacobian of Eqs. (4) and (8) vanishes, that is,

$$\begin{vmatrix} \frac{\partial x}{\partial r} & \frac{\partial x}{\partial \theta} \\ \frac{\partial y}{\partial r} & \frac{\partial y}{\partial \theta} \end{vmatrix} = 0 \tag{9}$$

Consequently, applications of Eq. (9) to the mapping equations (7) give the equations of the initial curves (10). The initial curves are circles, around the crack tip and the center of the hole, with fixed radii r_o. With the mapping equations (7) the caustic curves are finally obtained as images of the initial curves (10) and are given as shown in equations (11) in the table below.

Mathematically, the caustic curve at the crack tip is generalized epicycloids and around the center hole is classified as a nephroid as shown in Fig. 5. For the quantitative evaluation of caustics a length parameter between characteristics points on the caustic curve is defined, e.g., the maximum diameter of the caustic curve given by the maximum diameter D_{max} in Fig. 5. These distances are related to the radii of the initial curve by equations (12). With equations (9) and (12) a quantitative formula is obtained in each case relating the size of the reflected caustics pattern with mode one SIF (K_I) and the stress optical constant for central hole image, listed as equation 13.

Table 2: Mathematics and Engineering

Equation	Edge Crack	Circular Hole
3	$\sigma_1 + \sigma_2 = K_I \sqrt{\frac{2}{\pi r}} \cos\frac{\theta}{2}$	$\sigma_1 + \sigma_2 = \frac{\sigma}{2}\left(2 + \frac{4a^2}{r^2}\cos 2\theta\right)$
5	$D = \Gamma r^{-3/2} K_I \left(\cos\frac{\theta}{2}\,\boldsymbol{u} + \sin\frac{\theta}{2}\,\boldsymbol{v}\right)$	$D = \Gamma r^{-3}(\cos 2\theta\,\boldsymbol{u} + \sin 2\,\theta\,\boldsymbol{v})$
6	where $\Gamma = \frac{Z_o dc}{\sqrt{2\pi}}$	$\Gamma = 4Z_o c d\sigma a^2$
8	$r^{/} = \left(r cos\theta + \Gamma K_I\, r^{-3/2} \cos\frac{3}{2}\theta\right)\boldsymbol{i}$ $+\left(r sin\theta + \Gamma K_I\, r^{-3/2} \sin\frac{3}{2}\theta\right)\boldsymbol{j}$	$r^{/} = (r cos\theta + \Gamma r^{-3}\cos 3\theta)\mathbf{i}$ $+(r sin\theta + \Gamma r^{-3}\sin 3\theta)\mathbf{j}$
10	$r_{oc} = \left(\frac{3\Gamma}{2\lambda} K_I\right)^{2/5}$	$r_{oh} = \left(\frac{3\Gamma}{\lambda}\right)^{1/4}$
11	$x^{/} = \lambda r_{oc}\left(cos\theta + \frac{2}{3} cos\frac{3}{2}\theta\right)$ $y^{/} = \lambda r_{oc}\left(sin\theta + \frac{2}{3} sin\frac{3}{2}\theta\right)$	$x^{/} = \lambda r_{oh}\left(\cos\theta + \frac{1}{3}\cos 3\theta\right)$ $y^{/} = \lambda r_{oh}\left(sin + \frac{1}{3}\sin 3\theta\right)$
12	D_{max}=3.17 r_{oc}	D_{max}=2.67 r_{oh}
13	$K_I = \frac{2\sqrt{2\pi}}{3(3.17)^{5/2} Z_o d\boldsymbol{C}} D_{max}{}^{5/2}$	$\boldsymbol{C} = \frac{F}{12(2.67)^4 Z_o dAa^2} D_{max}{}^4$

EXPEREMENTS

The experimental arrangement of the method is simple as shown in Fig. 6. A convergent, or divergent, light beam impinges on the specimen in the close vicinity of the crack tip/hole and the reflected rays are received on a reference plane, parallel to the plane of the specimen. These rays, due to the thickness and refractive index variations in the region close to the crack tip/hole, are reflected in a dispersive way. Some of these rays are concentrated along a strongly illuminated curve on the reference plane, which is placed at some distance Z_o from the specimen. This is called a caustic.

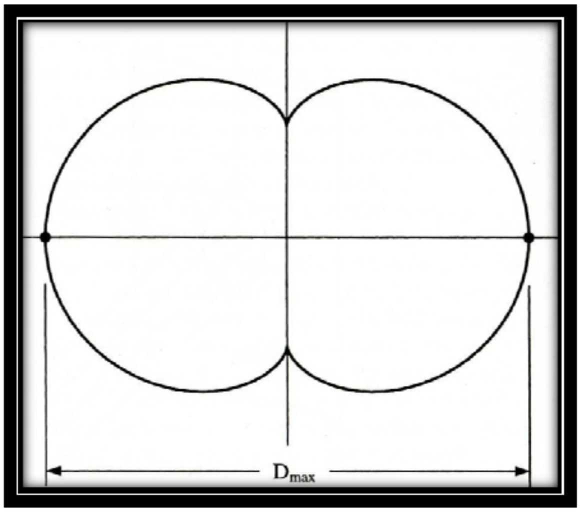

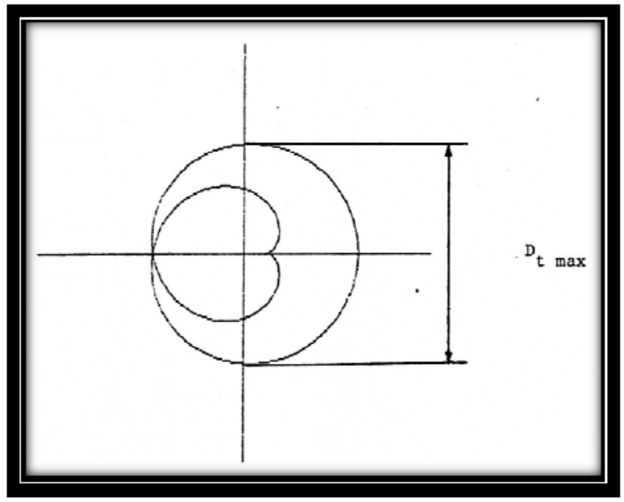

Figure 5 Theoretical caustics for central hole and edge crack

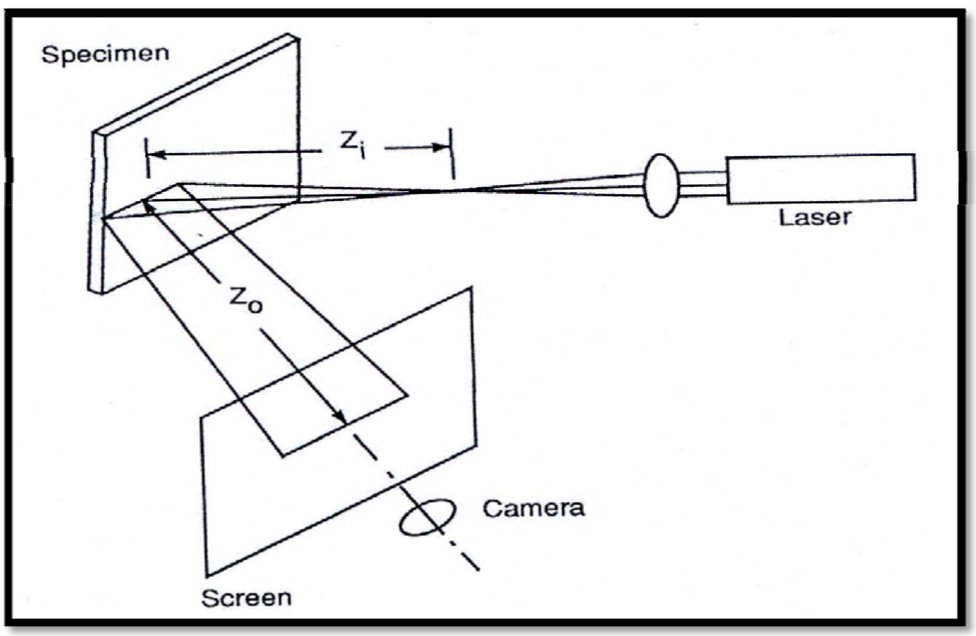

Figure 6 Experimental arrangement of the reflected caustics method

The method of reflected caustics was applied to a thin plate containing an edge crack (6.5mm) and subjected to a uniaxial load at distance from the crack. The material of the plate was plexiglass since it is mechanically and optically isotropic material. The method was also applied to a plate from the same plexiglass sheet (230x40x3.3mm), but with a central hole of 3 mm diameter. A monochromatic light beam emitted from a He-Ne laser was used as the light source. All models were loaded in tension to a level below the yield strength of the material. The resulting reflected caustics images are shown in figure 7.

The inner caustics are the results of the light reflecting from the front face whereas the outer ones are due to the light reflecting from the rear face of the specimens. Furthermore, the reflected caustic from the front face is related to the mechanical properties of the material and the outer caustics are related to the mechanical as well as the optical properties of the material. The light rays are deviated outwards. Thus, the crack tip, central hole, and the initial curves cannot be seen on the caustic images. It was observed that the experimental inner crack caustic is not closed. This is due to the crack opening displacement.

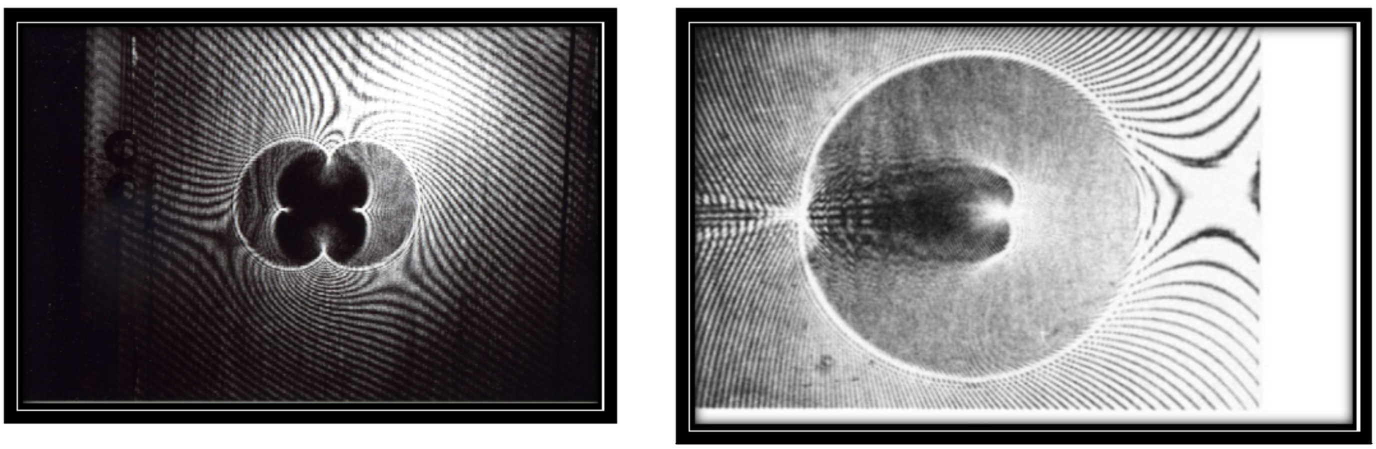

Central Hole *Edge Crack*

Figure 7 Experimental reflected caustics images

RESULTS

Mode one stress intensity factor can be determined by measuring the maximum transverse diameter (equation 13). However, it was noticed during the experiments that the caustic rim in figure 7 has a band shape rather than a fine line of figure 5. This is due to the light diffraction effects. The literature is inconclusive regarding the measurement D_{max} for transmitted caustic (laboratory type) as outlined in reference [11]. Surprisingly, this issue has not been investigated about the reflected caustic yet. The author is attempting to address this issue about the reflected caustic (practical application) here.

In practice the actual light intensity at the caustic is bounded and the diffraction effects make the measurement of the diameter ambiguous. It is worth noting at this point that K_I varies as a 5/2 power of the caustic diameter. Thus, the effects of diffraction on the measurement of the caustic diameter are examined in this article in detail. This will account for the wave-optics aspects, light intensity. A digital image analysis system was used to study the light distribution across the maximum caustics diameters as shown in Fig. 8.

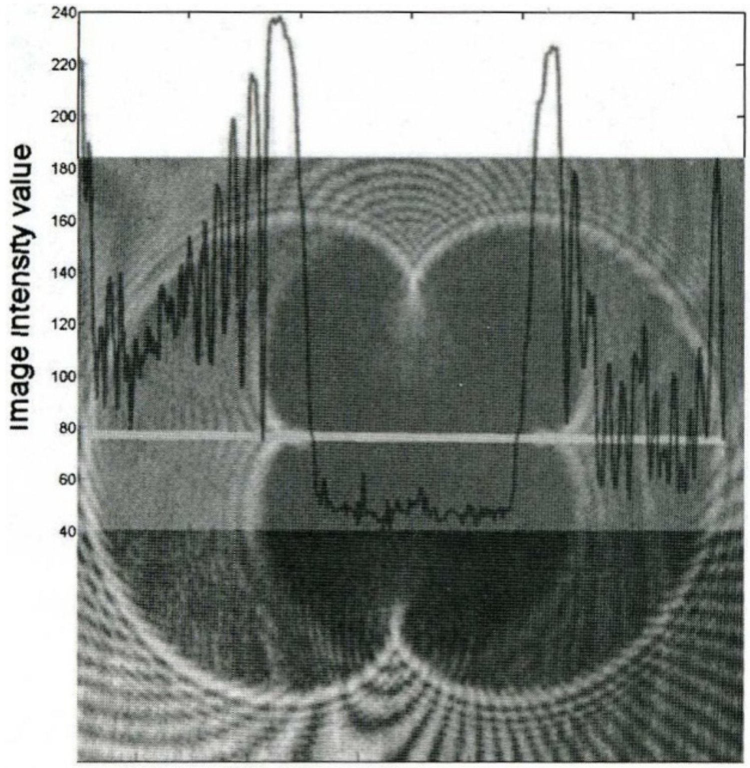

Figure 8 Distribution of light intensity

One school of thought measures the diameter as the outside of the black spot whereas another group suggests the diameter corresponding to the maximum light intensity, and some researchers use the outside diameter. The three diameters used to calculate K_I are listed in Table 3. First, K_I was calculated using the stress optical constants that are available in the literatures (C_1 = 3.30 x$10^{-10}$and C_2 = 2.98 x10^{-10}) m^2/N. The references do not indicate what method was used to obtain C. Then, the experimental results are compared to the theoretical K_I value [17, 18]. The percentage difference between the experimental values and the theoretical one is listed in Table 3. It is clear that uncertainty controls the results.

Second, the proposed calibration technique was used to determine the stress optical constant utilizing the center hole caustic. The three diameter were considered to calculate the stress optical constant (C) from equation 13. Subsequently, K_I was calculated based on the corresponding stress optical constant value. For example, the stress optical constant was determined based on the maximum light intensity diameter and its value was used in calculating K_I based on the maximum light transverse diameter. The results for this proposed technique are shown in table 3. It appears that the proposed technique clears the current ambiguity in regard to using the reflected caustic in the fracture mechanics field.

Table 3: Percentage difference results

Diameter	Based on C_1	Based on C_2	Proposed technique
Inner	-7.64	+3.16	-2.43
Maximum light intensity	+7.37	+16.17	+1.73
Outer	+11.32	+21.45	+5.61

CONCLUSIONS

In this study, experimental results for determining mode one stress intensity factor at a crack tip using the method of reflected caustic are presented. The focus was on selecting the experimental epicycloids maximum diameter.

The uncertainty in selecting the maximum diameter or/and the stress optical constant was investigated. An extensive diffraction error analysis showed that an interaction between the different reflected caustic diameter and the stress optical constant produces amplification to the error of determining K_I.

Calculating K_I based on different diameters and the corresponding stress optical constant enhance the accuracy of the optical method of reflected caustic. The results obtained lead to the following conclusions:

- Better K_I results can be obtained if the inside diameter is considered as the maximum diameter.
- Regardless of the value of stress optical constant value, a large error of K_I results is obtained if the outside caustic diameter is used.
- As a by-product of this study one may state the importance of calibration in determining the stress intensity factor experimentally. It is essential that the stress optical constant must be determined experimentally and then used in K_I calculation.
- In spite of the diffraction effects, accurate K_I results are obtained if the same diameter from the hole caustic is used in calculating the stress optical constant.

REFERENCES

1. P. Manogg, (1964) “Anwendung der schattenoptic zur untersuchung des zerreibvorgangs von platen,” Dissertation. University of Freiburg, Germany.

2. P. S. Theocaris, (1981) "Elastic stress intensity factors evaluated by caustics," Mechanics of Fracture, 7, G.C. Sih, ed., Sijthoff and Noordhoff, The Hague.

3. T. Takanobu, (2006), “Development of measurement system using the caustics method based on database (application for measurement of contact load),” *Journal of Material Testing Research Association of Japan*, Vol. 51, pp. 77-83.

4. A. Bakić, D. Semenski1 and S. Jecić, (2010) “The caustics method in the contact problems of anisotropic materials,” *EPJ Web of Conferences*, Vol. 6.

5. V. Spitas, G. A. Papadopoulos, C. Spitas, T. Costopoulos, (2011) “Experimental investigation of load sharing in multiple gear tooth contact using the stress-optical method of caustics,” *Strain*, Vol. 47, pp. 227-233.

6 X. F. Yao and W. Xu, (2011) “Recent application of caustics on experimental dynamic fracture studies,” *Fatigue & Fracture of Engineering Materials & Structures*, Vol. 34, pp. 448-459.

7. I. R. Wallhead, S. Güngör, and L. Edwards, (1994), “Optimization of the optical method of caustics for the determination of stress intensity factors,” *Optics and Lasers in Engineering*, Vol. 20, pp. 109-133.

8. C.P. Spyropoulos, (2001) “Stress intensity factor determination error by the method of caustics,” *Theoretical and Applied Fracture Mechanics*, Vol. 35, pp. 179-186.

9. M. K. Gdoutos and E. E. Gdoutos, (1992) “Guidelines for applying the method of caustics in crack problems,” *Experimental Techniques*, Vol. 16, pp. 25-28.

10. G. A. Papadopoulos, (2011) “New formula of experimental stress intensity factor evaluation by caustics,” *International Journal of Fracture*, Vol. 171, pp. 79-84.

11. N.T. Younis, I. Miskioglu, and S.E. Egleston, (1994) “ Simple calibration method for determining K_I using the method of caustics,” *Optical Engineering,* Vol. 33, pp. 2964-2971.

12. R. A. Tomlinson and E. A. Patterson, (1999) “The effects of surface topography on the method of caustics,” *Experimental Mechanics*, Vol. 39, pp. 335-341.

13. N. T. Younis, (2002) “New optical method for determining Poisson’s ratio/Young’s modulus for transparent materials,” *Optical Engineering*, Vol. 41, pp. 471-478.

14. D. N. Pazis, Z. Agioutantis and S. K. Kourkoulis, (2011) “The optical method of reflected caustics applied for a plate with a central hole: critical points and limitations,” *Strain*, Vol. 47, pp. 489-498.

15. B. G. Badalouka and G. A. Papadopoulos, (2006) “Range of applicability of the method of caustics around holes,” *Strain*, Vol. 42, pp. 283-290.

16. N. T. Younis and L.W. Zachary, (1989) "A New technique for the determination of stress optical constants using the shadow-spot method," *Experimental Mechanics*, Vol. 29, pp. 75-79.

17. M. Janssen, J. Zuidema and R. Wanhill, Fracture Mechanics, Spon Press, New York (2004).

18. A. P. Boresi and R. J. Schmidt, Advanced Mechanics of Materials, John Wiley, New York (2003).

19. W. F. Riley, L. D. Sturges and D. H. Morris, Mechanics of Materials, John Wiley, New York (2007).

20. M. Born and E. Wolf, Principles of Optics, Pergamon Press, New York (1975).